NJC

PAPER

View Article Online
View Journal | View Issue

Cite this: *New J. Chem.*, 2019, 43, 16960

p-Nitro-tetradecyloxy-calix[4]arene as a highly selective stationary phase for gas chromatographic separations†

Tao Sun, *[a] Xiaomin Shuai,[b] Li Bin,[c] Kaixin Ren,[a] Xingxing Jiang,[a] Haipeng Chen,[a] Shaoqiang Hu[a] and Zhiqiang Cai*[b]

Received 23rd July 2019,
Accepted 8th October 2019

DOI: 10.1039/c9nj03813b

rsc.li/njc

Here, we report the first example of the utilization of *p*-nitro-tetradecyloxy-calix[4]arene (C4A-NO_2) as a stationary phase for capillary gas chromatographic (GC) separations. The statically coated C4A-NO_2 column exhibited a high column efficiency of 3815 plates per m and moderate polarity. The C4A-NO_2 column was investigated for its separation performance and retention behaviours by utilizing a wide variety of isomer mixtures, covering alkylated benzenes and naphthalenes, alkenes, furans, alcohols, benzaldehydes, phenols and halogenated anilines. Importantly, the C4A-NO_2 column exhibited high resolving capability for both aliphatic and aromatic isomers. Particularly, it displayed advantageous resolving capability over the commercial DB-17 column for halogenated aniline isomers. This work provides a good reference for designing calixarene derivatives as GC stationary phases, which is important for developing a family of stationary phases with specific selectivity.

1. Introduction

Calixarenes, the third generation of host supramolecules after crown ethers and cyclodextrins, are cavity-shaped cyclic oligomers consisting of phenol units linked *via* methylene bridges.[1,2] Calixarenes possess unique features such as a rigid electron-rich cavity, highly selective interactions with analytes *via* H-bonding, dipole–dipole, π–π and hydrophobic interactions, low toxicity and high chemical and thermal stability.[3,4] By taking advantage of the introduction of functional groups into the aromatic skeleton (on upper or lower rim), a wide variety of chemically modified calixarene derivatives have been synthesized.[5–7] From the perspective of separation science, there are a number of selective factors in the configuration of calixarenes such as 3D cavity, conformation and substituents.[8,9] Due to their unique structures and physicochemical properties, calixarenes have shown good potential as separation materials for chromatographic separations.[10–12]

GC has been widely used in petrochemical, environmental, food and pharmaceutical fields because of its inherent advantages of simplicity, selectivity, sensitivity, speed and low cost.[13–16] Mangia *et al.* first used *p-tert*-butylcalix[8]arene as a stationary phase in packed GC and studied its retention behaviour for alkanols, chlorinated hydrocarbons and aromatic compounds.[17] Mŭnk *et al.* studied the inclusion properties of *p-tert*-butylcalix-[4]arene by GC.[18] However, their applications of unsubstituted calixarene as GC stationary phases are restricted due to their high melting point and poor film-forming ability. Accordingly, calixarenes are usually used together with polysiloxanes either in physical mixtures or chemically grafted polymers in order to improve the column efficiency and separation performance.[19–21] So, the selectivity and retention behaviour of calixarene itself as a GC stationary phase are not clear.

This work presents the investigation of utilizing *p*-nitro-tetradecyloxy-calix[4]arene (C4A-NO_2) as a stationary phase for GC separations (Scheme 1). We introduced nonpolar long alkyl chains and polar nitro functional groups at the lower and upper rims of calix[4]arene, respectively, which can increase its column efficiency and selectivity based on improving the solubility and film-forming ability of the stationary phase. After it was statically coated onto a fused-silica capillary column, the C4A-NO_2 stationary phase was investigated regarding its column efficiency and polarity. Its separation performance was evaluated by utilizing more than a dozen isomer mixtures of diverse types. To our knowledge, this is the first report employing C4A-NO_2 as the stationary phase for GC separations.

[a] *College of Chemistry and Chemical Engineering, Henan Key Laboratory of Function-Oriented Porous Materials, Luoyang Normal University, Luoyang 471934, P. R. China. E-mail: suntao2226@163.com*
[b] *Liaoning Province Engineering Research Center for Fine Chemical Engineering of Aromatics Downstream, School of Petrochemical Engineering, Shenyang University of Technology, Liaoyang, 111003, Liaoning, P. R. China. E-mail: kahongzqc@163.com*
[c] *Hebei Key Laboratory of Heterocyclic Compounds, Handan University, Handan 056005, P. R. China*

† Electronic supplementary information (ESI) available. See DOI: 10.1039/c9nj03813b

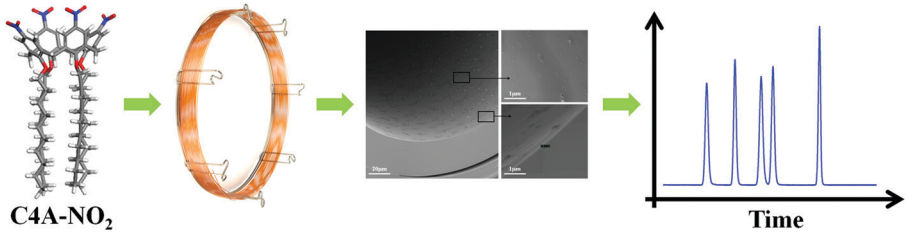

Scheme 1 The C4A-NO_2 capillary column for GC separation.

2. Experimental

2.1 Materials and equipment

All the reagents and solvents were commercially available without any further purification. All the analytes were of analytical grade and dissolved in dichloromethane. Untreated fused-silica capillary tubing (0.25 mm, i.d.) was purchased from Yongnian Ruifeng Chromatogram Apparatus Co., Ltd (Hebei, China). The commercial capillary column DB-17 (30 m × 0.25 mm, i.d., 0.25 μm film thickness, 50% phenyl 50% dimethyl polysiloxane) was purchased from Agilent Technologies and used as the reference column.

An Agilent 7890A gas chromatograph equipped with a split/splitless injector, a flame ionization detector (FID) and an auto-sampler was used for GC separations. All the separations were performed under the following GC conditions: nitrogen of high purity (99.999%) as carrier gas, injection port at 300 °C, split ratio at 60 : 1, and FID at 300 °C. Oven temperature programs for the GC separations were individually provided in their figure captions. ^{1}H NMR spectra were recorded using a Bruker Biospin 400 MHz spectrometer with TMS as the internal standard. All chemical shifts were reported in ppm. IR spectra were recorded using a Bruker Platinum ART Tensor II FT-IR spectrometer. MALDI-7090 TOF-MS was recorded using a Bruker BIFLEX III mass spectrometer. Thermogravimetric analysis (TGA) was performed using a DTG-60AH instrument (Shimadzu, Japan). Scanning electron microscopy (SEM) images were recorded using a Zeiss Sigma 500 microscope (Zeiss, Germany).

2.2 Synthesis of the C4A-NO_2 stationary phase

C4A-NO_2 was synthesized according to references and its synthetic procedure is outlined in Fig. 1.[22,23] *para* tertiary butyl phenol (5.0 g, 0.03 mol) was dissolved in 40% formaldehyde solution (30 mL, 0.04 mol), and sodium hydroxide (0.06 g, 1.5 mmol) was added to it. The mixture was stirred at 120 °C for 2 h and diphenyl ether (50 mL) was added dropwise. After stirring for 5 h at the same temperature, the mixture was cooled down to room temperature and then ethyl acetate (50 mL) was added to it. There was a large amount of precipitation. After removal of the precipitate by filtration, a white solid was obtained. The white solid (1.5 g, 2.3 mmol) and 60% sodium hydrogen (1.0 g, 25 mmol) were dissolved in anhydrous DMF (15 mL). The mixture was stirred at room temperature for 0.5 h and *n*-$C_{10}H_{21}Br$ (20 mL) was added. The solution was heated to 85 °C for 6 h. A white precipitate began to precipitate out. The excess sodium hydrogen was decomposed by water and methanol. A solid (1.5 g, 1.2 mmol) was obtained by filtering, which was dissolved in CH_2Cl_2 (90 mL) and ice acetic acid (15 mL), then the solution was cooled to 0 °C, and 95% fuming nitric acid (5 mL) was added to the mixture. After stirring for 0.5 h, the mixture was raised to room temperature until the reaction was completed. The reaction mixture was diluted with water, and the organic phase was dried over anhydrous sodium sulfate, filtered, and concentrated *in vacuo* to give the crude product as a yellow powder. ^{1}H NMR ($CDCl_3$, 400 MHz): δ 8.29–7.64 (m, 8H), 4.29–4.08 (m, 8H), 4.01–3.75 (m, 8H), 1.76 (s, 8H), 1.24 (dd, J = 16.8, 11.6 Hz, 56H), 0.85 (t, J = 6.8 Hz, 12H); IR (KBr, cm^{-1}): 2920 (C–H), 2850 (C–H), 1640 (C═C), 1580 (C═C), 1520 (C═C), 1450 (C═C), 1340 (N–O), 1260 (C–O–C), 1230 (C–O–C), 1090 (C–O–C), 748 (C–H); MALDI-TOF MS: m/z calcd for $C_{68}H_{108}N_4O_{12}$: 1164.7338 (100%); found: 2352.4543 $[2M + Na]^+$ (100%).

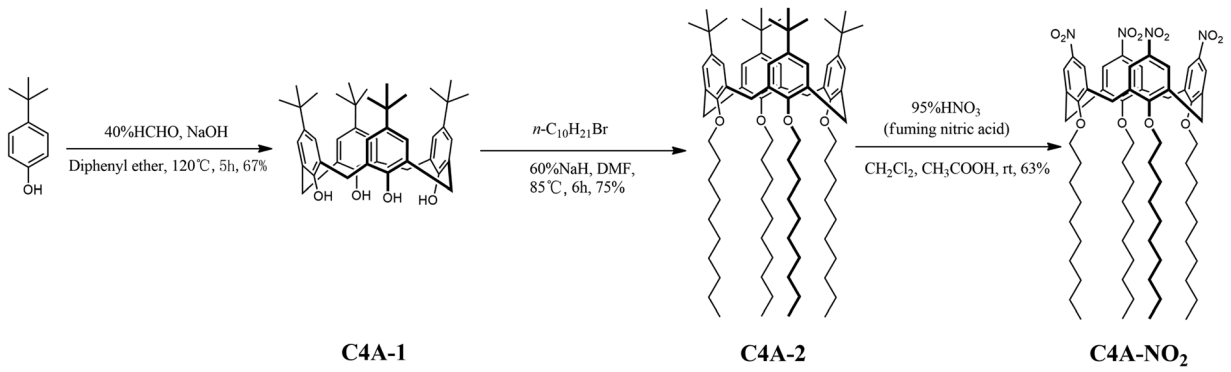

Fig. 1 Synthesis of C4A-NO_2.

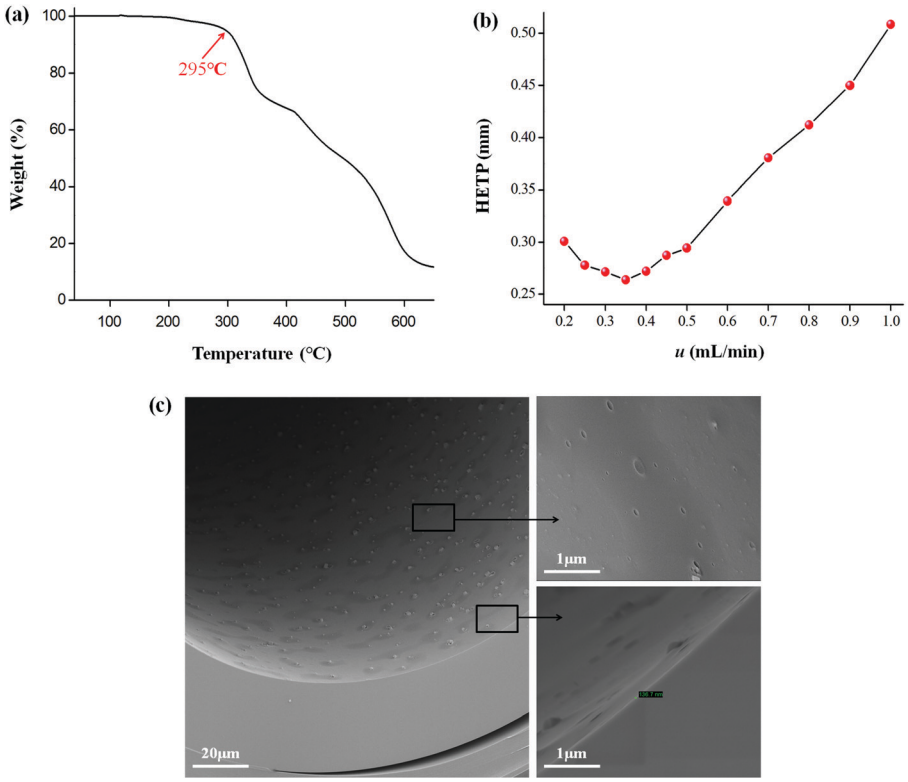

Fig. 2 (a) TGA plot for the C4A-NO_2 stationary phase from 40 °C to 600 °C at 10 °C min^{-1}; (b) Golay plot of the C4A-NO_2 column determined by using *n*-dodecane at 120 °C; (c) the cross-section SEM images on the inner wall surface and the coating of the C4A-NO_2 column.

2.3 Fabrication of the C4A-NO_2 capillary column

The C4A-NO_2 capillary column was fabricated by using the static coating method.[24,25] Before coating, one bare fused-silica capillary column (10 m × 0.25 mm, i.d.) was pretreated with a saturated solution of sodium chloride in methanol for the inner surface roughening of the capillary column. Then, the solution was removed and the column was conditioned up to 200 °C and held for 3 h under a nitrogen atmosphere. After the pretreatment, the column was statically coated with the solution of the C4A-NO_2 stationary phase in dichloromethane (0.15%, w/v) at room temperature. After the column was filled with the coating solution and sealed at one end, the solvent was evaporated at a steady speed from the other end under vacuum. Finally, the column was conditioned from 40 °C to 180 °C at 1 °C min^{-1} and

Table 1 McReynolds constants of the C4A-NO_2 and commercial column

Stationary phases	X′	Y′	Z′	U′	S′	General polarity	Average
C4A-NO_2	92	179	155	241	214	881	176
DB-17	154	134	176	266	218	948	190

X′, benzene; Y′, 1-butanol; Z′, 2-pentanone; U′, 1-nitropropane; S′, pyridine. Temperature: 120 °C.

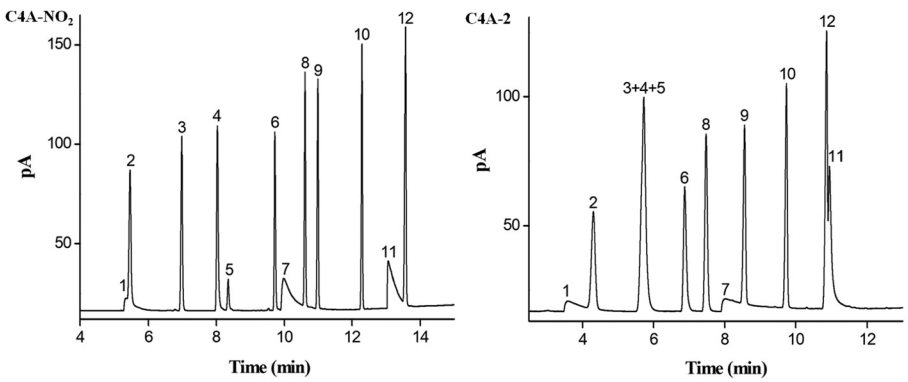

Fig. 3 Separations of the Grob mixture on the C4A-NO_2 column in comparison to the C4A-2 column. Peaks: (1) 2,3-butanediol, (2) *n*-decane, (3) *n*-undecane, (4) 1-octanol, (5) *n*-nonanal, (6) 2,6-dimethylphenol, (7) 2-ethylhexanoic acid, (8) 2,6-dimethylaniline, (9) methyl decanoate, (10) methyl undecanoate, (11) dicyclohexylamine, (12) methyl dodecanoate. Temperature program on C4A-NO_2 and C4A-2 columns: 40 °C for 1 min to 160 °C at 10 °C min^{-1}, and held at 160 °C for 3 min. Flow rate at 0.6 mL min^{-1}.

held at 180 °C for 7 h under nitrogen. The as-prepared C4A-NO_2 column was used for the following work. By using the same procedure, the C4A-2 column was also obtained.

3. Results and discussion

3.1 Column efficiency and Golay plot

The C4A-NO_2 stationary phase was evaluated for its inherent thermal stability and polarity by thermal gravimetric analysis (TGA). As shown in Fig. 2a, C4A-NO_2 remains thermally stable up to 295 °C, suggesting its good thermal stability as a stationary phase for GC separations. For the fabricated C4A-NO_2 column, the Golay plot relating the heights equivalent to a theoretical plate (HETP) with flow rates was determined by using *n*-dodecane at 120 °C and is shown in Fig. 2b. The Golay plot showed the minimum HETP of 0.26 mm at 0.35 mL min^{-1}, corresponding to a column efficiency of 3815 plates per m. The high column efficiency can be attributed to the good solubility

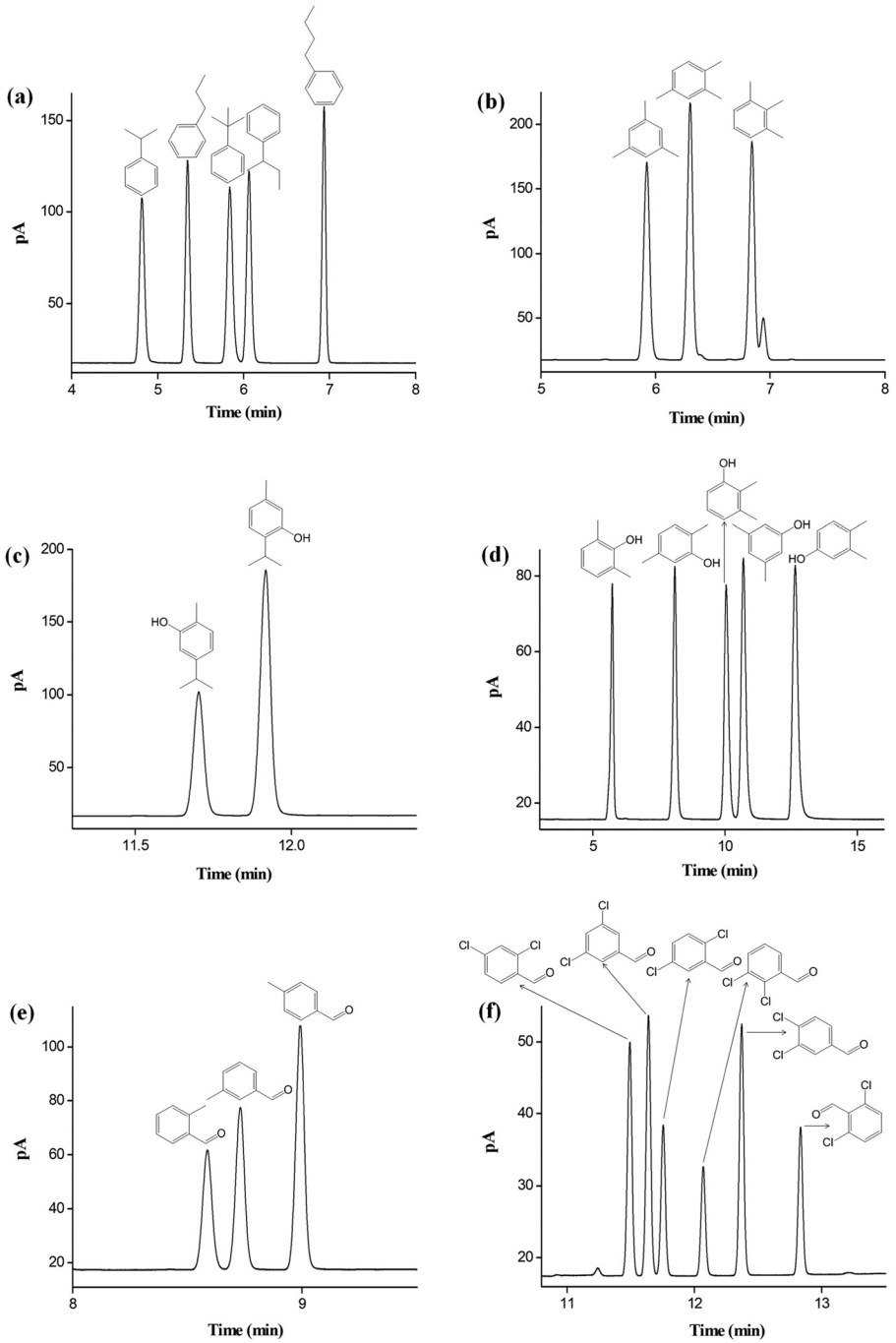

Fig. 4 Separations of isomer mixtures of (a) propylbenzene and butylbenzene, (b) trimethylbenzene, (c) carvacrol/thymol, (d) xylenol, (e) methylbenzaldehyde, and (f) dichlorobenzaldehyde on the C4A-NO_2 column. Temperature program: 40 °C for 1 min to 160 °C at 10 °C min^{-1} for (a), (b), (c) and (e). Temperature program: 40 °C for 1 min to 160 °C at 10 °C min^{-1} for (d) and (f), and held at 160 °C for 3 min. Flow rate at 0.6 mL min^{-1}.

of the C4A-NO_2 stationary phase in the solvent for column fabrication, facilitating its uniform coating on the capillary wall. In addition, the SEM images of the cross section and the inner coating of the C4A-NO_2 capillary column are shown in Fig. 2c, respectively, confirming its uniform coating with the thickness of approximately 136 nm on the capillary column.

3.2 McReynolds constants and polarity

Polarity of a stationary phase provides important chromatographic information for its selectivity and retention behaviours in GC separations. It can be evaluated by using the McReynolds constants of five probe compounds, *i.e.*, benzene (X′), 1-butanol (Y′), 2-pentanone (Z′), 1-nitropropane (U′) and pyridine (S′) at 120 °C.[26,27] The general polarity and average polarity were obtained by the sum and average of these five McReynolds constants, respectively. Table 1 lists the McReynolds constants of the C4A-NO_2 stationary phase, suggesting its moderate polarity close to that of the DB-17 phase. For this reason, we chose the DB-17 phase as the reference for the following investigation.[28]

3.3 Separation of the Grob test mixture

The Grob test mixture containing 12 analytes is well-recognized for comprehensive evaluation of separation performance of a GC column and a chromatographic system. Some of the analytes are quite tough to resolve from their adjacent analytes. Fig. 3 shows the GC separation of the Grob mixture on the C4A-NO_2 and C4A-2 columns. As shown, generally, the C4A-NO_2 column achieved better resolution and peak shape for the analytes in the mixture than the C4A-2 column that coeluted the pair of *n*-undecane/1-octanol/*n*-nonanal (peaks 3/4/5) with similar boiling points (b.p. 191–196 °C). As demonstrated, the polar groups were connected to the upper rim of the C4A-NO_2 stationary phase to improve their selectivity and resolving capacity, due to the hydrogen bonding and dipole–dipole interaction between stationary phase and analytes. In addition, prolonged retention for 2-ethylhexanoic acid (peak 7) and dicyclohexylamine (peak 11) occurred on the C4A-2 phase probably due to their strong interaction with the few exposed silanol groups on the C4A-2 column, leading to the reversal in elution orders of 2-ethylhexanoic acid/2,6-dimethylaniline

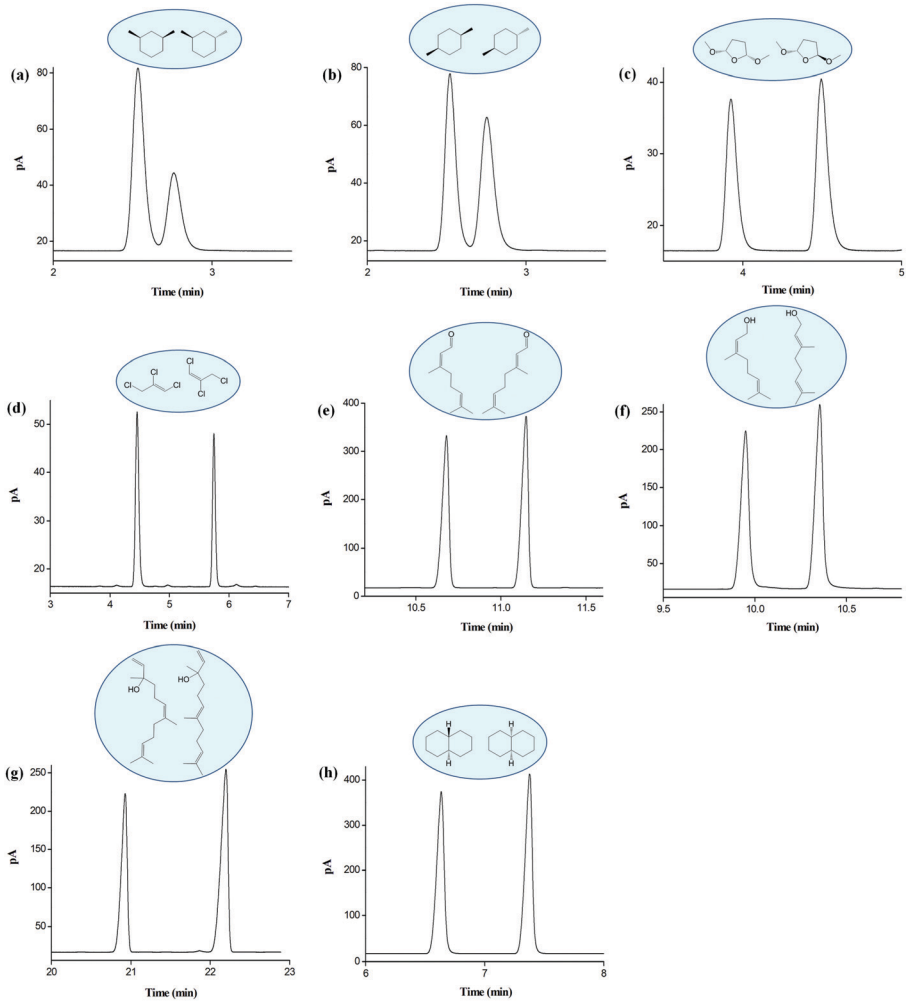

Fig. 5 Separations of *cis*-/*trans*-isomers of (a) 1,3-dimethylcyclohexane, (b) 1,4-dimethylcyclohexane, (c) 2,5-dimethoxytetrahydrofuran, (d) 1,2,3-trichloropropene, (e) citral, (f) nerol/geraniol, (g) nerolidol, and (h) decahydronaphthalene on the C4A-NO_2 column. Temperature program for (a), (b), (c), (d), (e), (f) and (h): 40 °C (1 min) to 160 °C at 10 °C min^{-1}; temperature program for (g): 40 °C (1 min) to 160 °C at 10 °C min^{-1}, and held at 160 °C for 10 min. Flow rate at 0.6 mL min^{-1}.

(peaks 7/8) and dicyclohexylamine/methyl dodecanoate (peak 11/12). The above results evidenced that the C4A-NO_2 column has better column inertness and separation performance for the tough analytes than the C4A-2 column. For such acids and amines, derivatization with appropriate reagents is often required to improve their peak shapes and resolution prior to their GC analysis.

3.4 Separation of structural, positional and *cis*-/*trans*-isomers

High-resolution separation of isomers is of vital importance in chemical industry and environmental analysis. It is also challenging to separate compounds with close boiling points and molecular masses in separation science. On the basis of its unique structural features, we undertook investigations on the resolving capability of the C4A-NO_2 stationary phase for a wide range of isomers. Fig. 4a–f shows the separations of six structural and positional isomers ranging from nonpolar to polar nature on the C4A-NO_2 column. As shown, the C4A-NO_2 column achieved baseline resolution for all the isomer mixtures with good peak shapes ($R > 1.5$), demonstrating its extraordinary high resolving ability for the critical analytes. Fig. 4a and b present the separation of propylbenzene, butylbenzene and trimethylbenzene isomers on the C4A-NO_2 column with high resolution, and the analytes eluted in order of their boiling points. The advantageous separation performance may be attributed to the cooperation of π–π and dispersion interactions between the 3D aromatic skeleton of calixarene and nonpolar aromatic analytes. Also, we examined the separation capability of the C4A-NO_2 column for polar aromatic isomers, such as phenols and benzaldehydes, which are susceptible to severe peak tailing and hard to resolve well. For carvacrol/thymol and

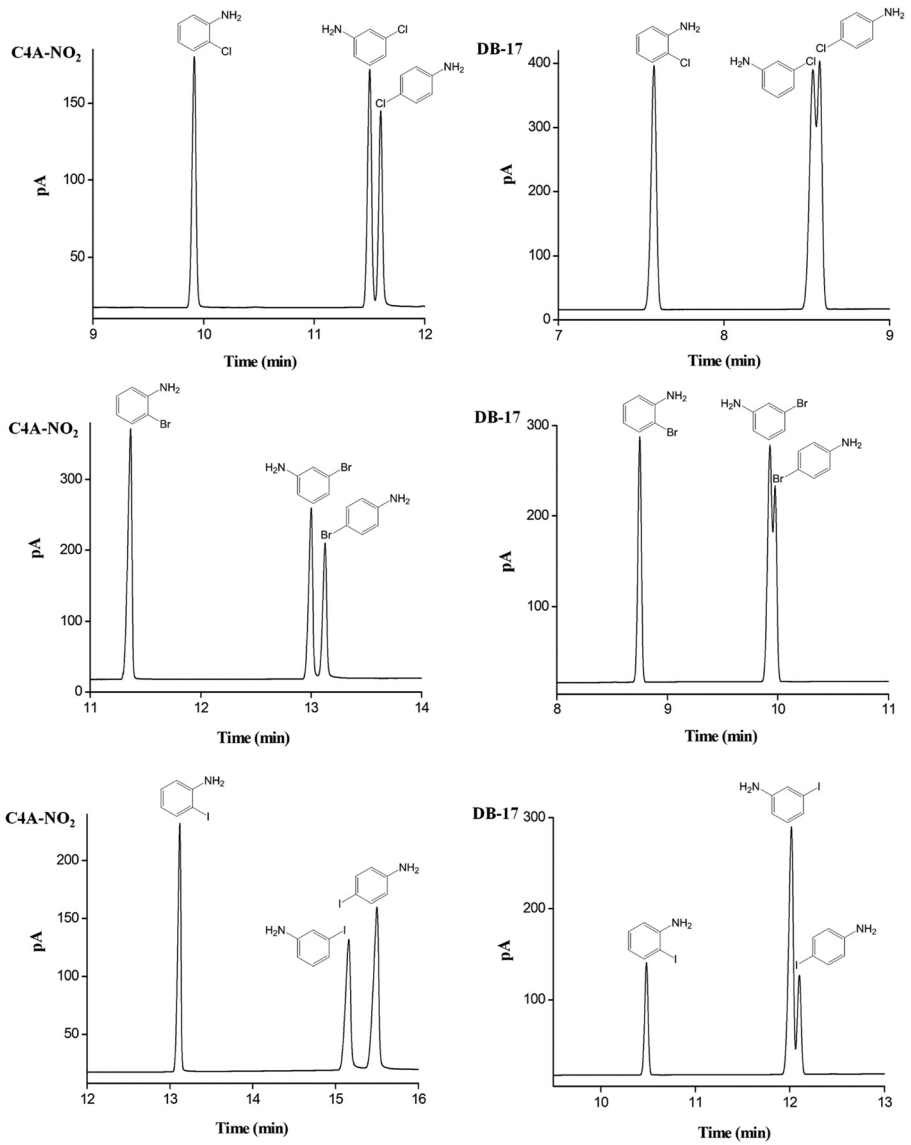

Fig. 6 Separations of halogenated aniline isomers on the C4A-NO_2 column in comparison to the DB-17 column. Temperature program on the C4A-NO_2 column (10 m): 40 °C for 1 min to 160 °C at 10 °C min^{-1}, and held at 160 °C for 3 min; temperature program on the DB-17 column (30 m): 120 °C for 1 min to 160 °C at 10 °C min^{-1}, and held at 160 °C for 8 min. Flow rate at 0.6 mL min^{-1}.

xylenols isomers in Fig. 4c and d, the C4A-NO_2 column exhibited baseline separation with symmetric peaks, suggesting its high resolving ability for polar analytes. It is noteworthy that thymol (b.p., 232 °C; 1.36 D) was eluted later due to its stronger H-bonding and dipole–dipole interactions with the stationary phase than carvacrol (b.p., 236 °C; 1.34 D). For the methylbenzaldehyde and dichlorobenzaldehyde isomers in Fig. 4e and f, the C4A-NO_2 column also achieved complete separations. Among them, the C4A-NO_2 stationary phase achieved good resolution for the critical pair of 2-methylbenzaldehyde (b.p., 200 °C) and 3-methylbenzaldehyde (b.p., 199 °C) with only a 1 °C difference in their boiling points. As for the elution order, the methylbenzaldehyde isomers follow the order of their extent of H-bonding and dipole–dipole interactions (2-methylbenzaldehyde, 3.72 D; 3-methylbenzaldehyde, 4.04 D; 4-methylbenzaldehyde, 4.12 D), similar to the case of carvacrol/thymol described above. Based on the above findings, we further explored the resolving capability of the C4A-NO_2 column for eight groups of *cis*-/*trans*-isomers, including 1,3-dimethylcyclohexane, 1,4-dimethylcyclohexane, 2,5-dimethoxytetrahydrofuran, 1,2,3-trichloropropene, citral, nerol/geraniol, nerolidol, and decahydronaphthalene. As displayed in Fig. 5, the C4A-NO_2 column also exhibited high resolution for geometric *cis*-/*trans*-isomers and showed good peak shapes, suggesting its high selectivity for both aliphatic and aromatic isomers with varying polarities. The above results evidence the high resolving performance of the C4A-NO_2 column for diverse types of isomers, which can be ascribed to its unique structure and multiple molecular interactions involving H-bonding, dipole–dipole, π–π and dispersion interactions.

Aromatic amine is a relatively important pollutant in the field of environmental analysis.[29,30] The efficient separation of aniline isomers is a big challenge in chromatographic separations.[31,32] Fig. 6 presents the separations of the chloroaniline, bromaniline and iodoaniline isomers on the C4A-NO_2 column in comparison to the DB-17 column. As shown, the C4A-NO_2 column well resolved the halogenated aniline isomers and showed advantageous separation capability over the DB-17 column. Notably, some of the analytes overlapped on the polysiloxane column. Moreover, the elution order of halogenated aniline isomers on the C4A-NO_2 stationary phase is consistent with the order of their polarity (*ortho* < *meta* < *para*). Regarding the driving forces for the separations, the H-bonding and dipole–dipole interactions mainly contribute to the resolution of the halogenated aniline isomers.

4. Conclusions

In this work, we present the first example of utilizing C4A-NO_2 as a stationary phase for GC separations. The C4A-NO_2 stationary phase exhibits excellent separation performance for diverse types of isomers, ranging from aliphatic to aromatic and from nonpolar to polar varieties. The high resolving capability of the C4A-NO_2 stationary phase may derive from its unique structure and comprehensive molecular interactions covering H-bonding, dipole–dipole, π–π and dispersion interactions. Most importantly, it shows high resolving ability for halogenated aniline isomers, showing advantages over the commercial polysiloxane phase. This work demonstrates the potential of the C4A-NO_2 stationary phase in GC and provides the basis for further investigation of more calixarene derivatives in chromatographic analysis.

Conflicts of interest

There are no conflicts to declare.

Acknowledgements

The work was supported by the National Natural Science Foundation of China (No. 21705072), Colleges and Universities in Henan Province Key Science and Research Project (No. 17A150039), and the Natural Science Foundation of Liaoning Province (20180550016).

References

1 S. Shinkai, *Tetrahedron*, 1993, **49**, 8933–8968.
2 K. Hyun Jung, L. M. Hee, M. Lucia, V. Jacques and K. Jong Seung, *Chem. Soc. Rev.*, 2012, **41**, 1173–1190.
3 M. Yilmaz and S. Erdemir, *Turk. J. Chem.*, 2013, **37**, 558–585.
4 O. Gezici and M. Bayrakci, *J. Inclusion Phenom. Macrocyclic Chem.*, 2015, **83**, 1–18.
5 P. Jose and S. Menon, *Bioinorg. Chem. Appl.*, 2007, 1–16.
6 S. P. Bew, R. A. Brimage, N. L'Hermite and S. V. Sharma, *Org. Lett.*, 2007, **9**, 3712–3716.
7 N. Natarajan, M. C. Pierrevelcin, D. Sémeril, C. Bauder, D. Matt and R. Ramesh, *Catal. Commun.*, 2019, **118**, 70–75.
8 S. B. Nimse and T. Kim, *Chem. Soc. Rev.*, 2013, **42**, 366–386.
9 B. T. Zhao, C. B. Wang, S. J. Wu and B. X. Ye, *Chin. J. Org. Chem.*, 2010, **30**, 1212–1219.
10 G. Delahousse, R. Lavendomme, I. Jabin, V. Agasse and P. Cardinael, *Curr. Org. Chem.*, 2015, **19**, 2237–2249.
11 W. J. Zhao, K. Hu, C. J. Wang, S. Liang, B. L. Niu, L. J. He, K. Lu, B. X. Ye and S. S. Zhang, *J. Chromatogr. A*, 2012, **1223**, 72–78.
12 K. Hu, W. F. Zhang, H. X. Yang, Y. X. Cui, J. Y. Zhang, W. J. Zhao, A. J. Yu and S. S. Zhang, *Talanta*, 2016, **152**, 392–400.
13 B. J. Pollo, G. L. Alexandrino, F. Augusto and L. W. Hantao, *TrAC, Trends Anal. Chem.*, 2018, **105**, 202–217.
14 A. M. Muscalu and T. Górecki, *TrAC, Trends Anal. Chem.*, 2018, **106**, 225–245.
15 M. V. Russo, P. Avino, L. Perugini and I. Notardonato, *RSC Adv.*, 2015, **5**, 37023–37043.
16 C. Citti, D. Braghiroli, M. A. Vandelli and G. Cannazza, *J. Pharm. Biomed. Anal.*, 2018, **147**, 565–579.
17 A. Mangia, A. Pochini, Ŕ. Ungaro and G. D. Andreetti, *Anal. Lett.*, 1983, **16**, 1027–1036.
18 P. Mňuk and L. Feltl, *J. Chromatogr. A*, 1995, **696**, 101–112.
19 B. Gross, J. Jauch and V. Schurig, *J. Microcolumn Sep.*, 1999, **11**, 313–317.
20 X. H. Lai, L. Lin and C. Y. Wu, *Chromatographia*, 1999, **50**, 82–88.

21 Z. R. Zeng, N. Guan, X. H. Tang and X. R. Lu, *Analyst*, 2000, **125**, 843–848.
22 H. Hong, D. M. Li, W. Z. Wang, Y. C. Chen, K. Khan, S. Song and Y. S. Zheng, *Org. Biomol. Chem.*, 2012, **10**, 729–735.
23 P. Shahgaldian, M. A. Sciotti and U. Pieles, *Langmuir*, 2008, **24**, 8522–8526.
24 Y. Zhang, M. L. Qi and R. N. Fu, *RSC Adv.*, 2016, **6**, 36163–36170.
25 J. Peng, T. Sun, L. Wu, M. Qi and X. Huang, *RSC Adv.*, 2017, **7**, 45408–45415.
26 X. H. Yang, C. X. Li, M. L. Qi and L. T. Qu, *RSC Adv.*, 2017, **7**, 32126–32132.
27 T. Sun, H. Chen, X. Qiao, L. Ma, S. Hu and X. Liu, *RSC Adv.*, 2018, **8**, 34102–34109.
28 C. Ragonese, D. Sciarrone, P. Q. Tranchida, P. Dugo and L. Mondello, *J. Chromatogr. A*, 2012, **1255**, 130–144.
29 H. Kataoka, *J. Chromatogr. A*, 1996, **733**, 19–34.
30 T. C. Schmidt, R. Haas, K. Steinbach and E. von Löw, *Fresenius' J. Anal. Chem.*, 1997, **357**, 909–914.
31 M. Chen, G. Zhu, S. Wang, K. Jiang, J. Xu, J. Liu and J. Jiang, *J. Sep. Sci.*, 2018, **41**, 440–448.
32 S. S. Wang, Y. Y. Cheng, M. M. Chen and K. Z. Jiang, *Eur. J. Mass Spectrom.*, 2018, **24**, 337–343.